Application of Dielectric Measurements to Estimate Archie Parameters *m* and *n* from Drainage and Imbibition Data

Salah Al-Ofi[1,*], *Shouxiang* Ma[2], *Amer* Hanif[3] and *Fei* Le[3]

[1]Baker Hughes, Dhahran Technology Center 4.0, 31952 Dhahran, Saudi Arabia
[2]Saudi Aramco, Reservoir Description Division, 31952 Dhahran, Saudi Arabia
[3]Baker Hughes, Houston Technology Center, 2001 Rankin Rd, Houston, United States

Abstract. Archie equation is the foundation of modern petrophysics and parameters m, cementation exponent, and n, saturation exponent, are critical inputs of Archie equation. Traditionally, m and n are obtained from core analysis, which are available only in cored formations, and the process is costly and time consuming, especially for n which is known to be sensitive to rocks wettability and flooding cycle, drainage or imbibition. Multi-frequency dielectric data is used to derive m and n and its accuracy is investigated to assess its downhole applicability for different flooding regimes. To derive Archie m and n from multi-frequency dielectric data, we obtained dielectric constant using an open-ended coaxial laboratory test probe operating between 10 MHz and 1 GHz on clean outcrop core samples. For data interpretation, we used an approach which considers matrix, hydrocarbon and water as three different phases in dielectric data processing, by applying effective medium theory on the formation rock in two steps: first between water and hydrocarbon resulting in an effective fluid permittivity, then second between effective fluid permittivity and matrix. For validation purposes, we applied this technique on core samples after drainage and imbibition cycles and compare our dielectric results with m and n obtained from resistivity core analysis. The derived *m* and *n* from dielectric data from drainage core samples show good agreement with the core resistivity data. When compared with data from resistivity tests, the single-phase property m derived from the new method performs much better than that from *MN* approach. As for the two-phase property n from the primary drainage experiment, a significant improvement is also realized. The findings were consistent for different lithologies, sandstone and carbonate. As of forced imbibition experiment, n exponent shows insignificant hysteresis compared to drainage results as our samples are strongly water-wet and light mineral oil was used for cores desaturation. The derived *m* and *n* from dielectric data on imbibition experiments are comparable with core analysis data. However, m exponent derived from dielectric data showed better results from drainage experiment compared to imbibition. Using the new method presented in this study to interpret multi-frequency dielectric data has the potential to be implemented in interpreting downhole dielectric logs for continuous Archie parameters m and n, resolving a long-standing challenge in formation evaluation.

1 Introduction

1.1 Archie Parameters *m* and *n*

Since Archie published his work, the Archie model [1], eight decades ago, petrophysicists have been utilizing it heavily for formation evaluation from electrical logs. This Archie model, however, requires a prior knowledge of rock textural and fluid tortuosity parameters [2]; the cementation exponent *m* and saturation exponent *n* as following:

$$R_w/R_t = S_w{}^n \, \emptyset^m \quad (1)$$

Where R_t is the formation true resistivity, R_w is the formation brine resistivity, $\emptyset$ is porosity and S_w is water saturation. With known *m* and *n*, it is not only hydrocarbon reserves can be estimated using the above Archie model, but other fundamental formation properties, such as pore structure and permeability [3,4] and wettability [5] may also be characterized.

Conventionally, *m* and *n* are estimated either using core measurements [6], a time consuming and expensive process, or just assumed to be equal to some fixed value (such as the common default number of 2) which is rarely accurate particularly for complex reservoir rocks (such as lithology or texture) or fluids (such as crude oils with high polar components). In practice, *m* and *n* can vary both in-between and within zones often mandating different value inputs for a meaningful saturation from Archie or its derivative saturation algorithms. To enhance formation evaluation using the Archie model, a recent attempt was proposed to derive both *m* and *n* from multi-frequency dielectric measurement during the process of drainage of core samples [7].

1.2 Electrical Measurement Hysteresis

It is known that multiphase rock properties, such as Archie saturation exponent n, are sensitive to the history of fluid flow [8,9]. Hysteresis in electrical property of a porous rock is defined as the change of measured resistivity due to alteration of conducting fluid path geometry with respect to direction of saturation change in drainage and imbibition cycles.

* Corresponding author: salah.al-ofi@bakerhughes.com

There are several factors causing this hysteresis which have been reported. Moss et al. [8] reasoned the hysteresis in n estimation between drainage and imbibition is primarily due to wettability of the sample and wettability variation during changes in water saturation, as illustrated by the cartons of Ma et al. [6]. Their findings showed high hysteresis in *n* on cleaned reservoir samples compared to that of strongly water-wet outcrops [8]. Dernaika et al. [9] explained that the hysteresis between drainage and imbibition is due to fluids displacement mechanism, i.e. oil invasion in drainage occurs by piston-like when displacement pressure surpasses rock's capillary entry pressure, whereas for imbibition both piston-like and snap-off invasion mechanisms are possible. Snap-off displacement is more favorable when water content from the pore body corners is increased [10] or more swelling of films in water wet pores occurs resulting in trapped oil. This oil trapping phenomena is dependent on the shape of the fluid interface and aspect ratio between pore body and pore throat. Dernaika et al. [9] claimed that when larger aspect ratio of pore-throat is present in a rock, more snap-off displacement occurs and more hysteresis is expected. Their results implied that for imbibition on oil-wet samples after primary drainage occurred in which majority of adsorbed-water films were replaced by oil films, a piston-like displacement and less oil trapping is more favorable causing water to invades only large pores which are hydraulically disconnected. Thus, resistivity doesn't drop adequately to match the effect of increasing water saturation S_w in the Archie equation resulting in higher n for imbibition than that of drainage at same level of S_w [11].

For water-wet rocks, Tweheyo et al. [12] conducted relative permeability and resistivity index experiments on chalk samples and observed low values of *n* and small hysteresis and lower values for imbibition compared to drainage was reported. Some reported samples showed no hysteresis at all. The authors reasoned this behavior due to presence of fractures and micropores which conduct electrical current effectively even when large pores trap more oil. Another study conducted by Worthington and Pallatt highlighted the effect of microporosity and how it can alter default electrical current path with respect to saturation level and flow direction [13].

1.3 Archie's Parameters from Dielectric Measurement

Permittivity of a medium is defined as the amount of energy per unit volume stored or dissipated as electrical field passes through and expressed as a complex number:

$$\varepsilon_{\text{eff}}(\omega) = \varepsilon_r'(\omega) + i\varepsilon_r''(\omega) = \varepsilon_r'(\omega) + i\frac{\sigma(\omega)}{\omega\varepsilon_0} \quad (2)$$

Where
ε_{eff} is the effective permittivity of the mixture,
ε_r' is the real permittivity,
ε_r'' is the imaginary permittivity,
σ ($\sigma = 1/R_t$) is the conductivity in (Siemens/m),
ω is the angular frequency in (rad/second), and
ε_0 is the free-space (or vacuum) permittivity, i.e., 8.854x10^{12} (Farads/m).

Permittivity is a function of frequency. Measurement of formation permittivity at frequencies between 10 MHz and 1 GHz can be obtained by a group of transmitters and receivers that fire and receive electromagnetic waves [14, 15]. Deriving formation properties from dielectric dispersion data [16] depends on polarization mechanisms occurring during the measurement. In tens of MHz frequency range, it is dominated by interfacial polarization (Maxwell-Wagner), which occurs between any interface with a contrast in permittivity such as between solid grains and fluids, which can be modelled as water/oil and fluid/matrix interfaces. The polarization of both interfaces can be integrated in one mixing model to compute an effective permittivity [7].

Several models are available in the literature that computes the effective permittivity from a mixture of different constitutes. The most common model is CRIM, the Complex Refractive Index Model, by Birchak et al. [17] and modified to account for pore tortuosity by Forgang et al. [15]. Recently, Al-Ofi et al. [7] presented an interpretation model which can extract both Archie's exponents m and n from multi-frequency data simultaneously and independently, and the model was validated against outcrop core analysis data during drainage. One form of the model based on CRIM mixing method is expressed as follows:

$$\varepsilon_{eff}^{\frac{1}{m^*}} = \emptyset[S_w\varepsilon_w^{\frac{1}{n^*}} + (1-S_w)\varepsilon_o^{\frac{1}{n^*}}]^{\frac{n^*}{m^*}} + (1-\emptyset)\varepsilon_m^{\frac{1}{m^*}} \quad (3)$$

Where
$\emptyset$ is porosity of the medium,
m^* is cementation exponent as derived from dielectric model,
n^* is saturation exponent as derived from dielectric model,
S_w is water saturation,
ε_w is the permittivity of water,
ε_{oil} is the permittivity of oil, and
ε_m is the permittivity of solid matrix.

In this paper, we expand the work of Al-Ofi et al. [7] and investigate how dielectric data and its interpretation model's outputs can be influenced due to hysteresis in fluid flow by comparing the dielectric model's m^* and n^* with resistivity derived values using porous-plate core analysis.

2 Experiments

Since this is a continuation and expansion of Al-Ofi et al. [7], the methodologies and workflows between the two studies are similar. The focus of this study is to assess the hysteresis of fluid displacement on multi-frequency dielectric measurement by analyzing and comparing the Archie parameters obtained from the conventional resistivity method and dielectric method after drainage and imbibition cycles.

2.1 Experimental Procedures

The experimental plan and workflow are summarized in in Fig. 1. More details are elaborated below:

2.1.1 Core Preparation and Test Workflow

Procedures to prepare the core samples are listed below:

- Nine outcrop samples are cut to have 1.5 inches in diameter and 2 inches in length core plugs.
- Sister samples are prepared in smaller size, 1 inch in diameter and 1 inch in length for Mercury Injection Capillary Pressure (MICP) tests.
- The cores are cleaned using Sohxlet cells by toluene for one day at 110°C and then by methanol for 3 days at 60°C.
- After cleaning, the samples are transferred to a sonicator to clean out of debris resulted from core cutting and cleaning.
- Afterwards, cores were dried using a convection oven at 110°C for 1 day and finally put inside a desiccator while cooling down.
- Routine core analysis is then performed to obtain porosity, grain density, and permeability.

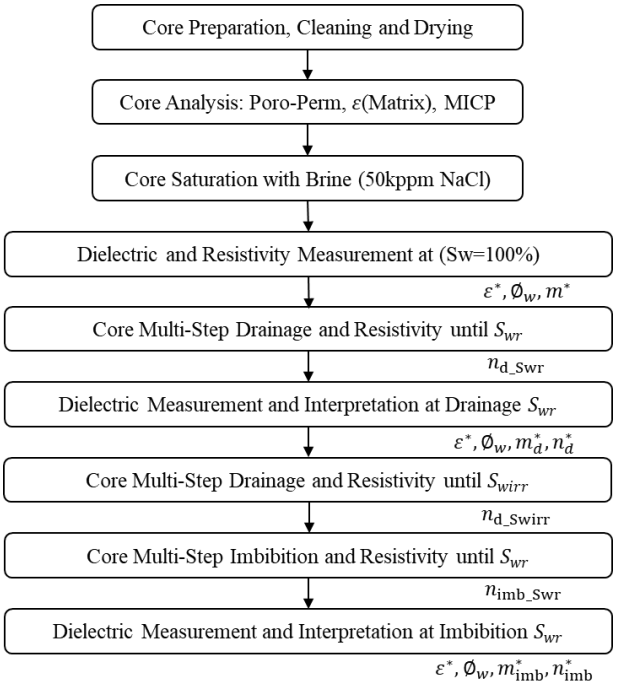

Fig. 1. Experimental validation workflow

2.1.2 Mercury Injection Capillary Pressure (MICP)

To characterize rock pore structure, MICP tests are conducted on the 1" by 1" core samples, in 110 pressure steps to a maximum pressure of 60,000 psi.

2.1.3 Dielectric Measurement

To ensure full water saturation of the 1.5" core plugs, the samples are mounted in a core holder and vacuumed for one day followed by an introduction of 50 kppm NaCl brine at 2,000 psi for another day

Dielectric data is obtained using an open-ended coaxial probe connected to Keysight Impedance analyzer (ENA series E4990A). The coaxial probe operates in a reflection mode [18] with S-parameter (S11) as the raw measurement, and the measurement frequency range is between 10 MHz and 1 GHz covering commercial dielectric logging tool band of frequencies [14,15]. The impedance analyzer is calibrated using a set of short, open, and 50 Ohm standards from Keysight. S11 parameter obtained by the coaxial probe is converted to complex dielectric constant $\varepsilon_{\mathrm{eff}}(\omega)$ [19]. The coaxial probe is calibrated using reference materials such as air and Teflon which have dielectric constants of 1 and 2.1, respectively. The dielectric measurement is obtained at atmospheric conditions and made by placing the coaxial probe at one flat end of a plug at a time. Average dielectric measurement of both ends of each core is considered for homogenous core samples. This procedure applies for samples at all saturation conditions.

2.1.4 Capillary Pressure Resistivity Index (PcRI)

Each 1.5" core plug is loaded into a core holder, at net confining stress of 2,000 psi, with a water-wet ceramic porous plate contacted by one end of the core plug. To avoid complexity of effect of wettability, a mineral oil is used. For drainage cycle, the mineral oil is injected into the fully water saturated sample at several capillary pressures corresponding to capillary pressure points as guided by the acquired MICP data on the sister 1" plugs. Similar capillary pressure points were used for the imbibition cycle, but with brine as injecting fluid and oil-wet ceramic porous plate at production side. An LCR meter, Keysight 4263B, records a 2-point resistance r_c across the sample's two ends at 20 kHz. The resistivity of the sample R_t is then obtained simply from the measurement of r_c, when the system reaches equilibrium [20,21].

2.2 Experimental Results and Discussions

2.2.1 Dry and Saturated Samples

Again, since this is a continuation and expansion of Al-Ofi et al. [7], the core samples used in the two studies are the same, as reported in Table 1 and Fig. 2. For fully brine saturated core samples, it has been shown that dielectric measurement are sensitive to water-filled porosity $\emptyset_w$ and cementation exponent m. Figure 3 and 4 show how the dielectric interpretation values generated from Bimodal mixing model, as defined in [22], are matching independently measured core data from gas porosity and resistivity.

Table 1. Dry samples measurements

Sample No	Lithology	Porosity (%)	Perm (mD)	ε_m
CO1-C	Sandstone	10.60	17.36	4.30
FB7-B	Sandstone	8.27	124.10	4.21
W-B	Dolomite	8.59	5.12	6.10
IL1-A	Dolomitic Lime	11.95	26.04	6.88
IL1-C	Limestone	18.41	195.80	7.58
IL3-A	Limestone	18.93	27.05	7.51
IL4-A	Limestone	19.86	126.12	7.57
IL4-B	Limestone	20.33	131.44	7.75
IL4-C	Limestone	20.51	163.50	7.57

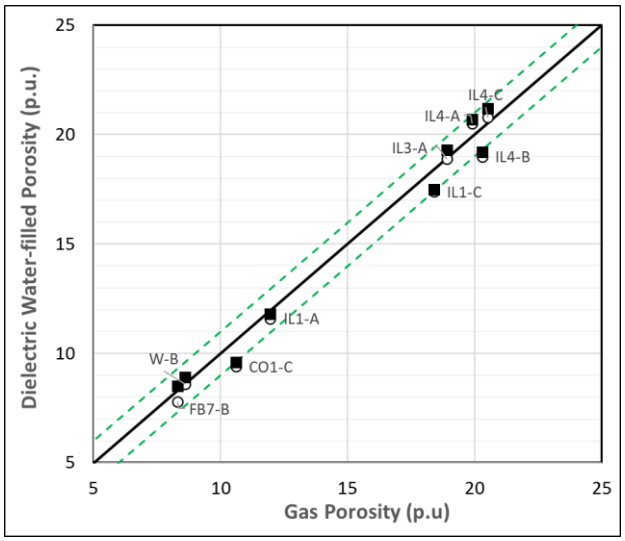

Fig. 3. At Sw=1, water-filled porosity using Bimodal model with $m = n$ (■) and $m \neq n$ (○), dashed lines indicate ±1 p.u. uncertainty. Water salinity is 50 kppm.

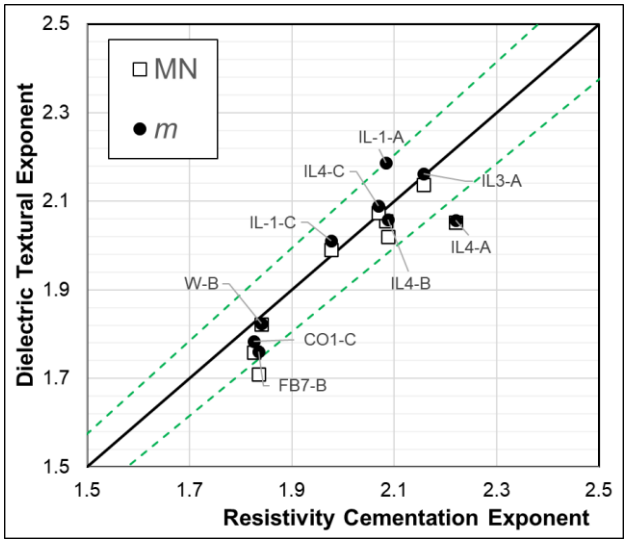

Fig. 4. At Sw=1, textural exponent from Bimodal model with $m = n$ (□) and $m \neq n$ and m (●), dashed lines indicate ±5% uncertainty. Water salinity is 50 kppm.

2.2.2 Drainage and Imbibition Measurements

As of downhole conditions, measurements of dielectric logging is shallow, detecting most likely the mud filtrate invaded regions, which is like imbibition in case of drilling with water-based mud (WBM) across a hydrocarbon interval. To validate the applicability of laboratory developed dielectric technique for downhole conditions, it's important to compare Archie's exponents derived from dielectric data obtained after imbibition cycle with resistivity-based exponents from imbibition PcRI tests and compare it with drainage cycle to assess the impact of drainage-imbibition hysteresis.

During drainage, the experiment was stopped to unload the core samples for dielectric measurement in a different set up at a specific water saturation S_{wr}, then the core sample was loaded back to core flooding system to continue the drainage process until reaching to irreducible water state S_{wirr}.

It is recognized that stopping a continuous drainage experiment is not the best practice, but is the best we can do with current laboratory capabilities to acquire both resistivity and dielectric permittivity on the same core at the same water saturation. Care was taken to carefully wrapped the core sample during loading and unloading process to minimize fluids loss. Nuclear Magnetic Resonance (NMR) T2 measurement is also used to monitor changes in water filled porosity at each step of loading and unloading.

After the drainage process, samples were unloaded and placed in brine filled Amott cell to obtain spontaneous imbibition before conducting imbibition test until the end of the imbibition test at which the samples were unloaded, and dielectric measurements were obtained.

2.2.3 Hysteresis Effect on Resistivity

Figures 5 and 6 demonstrate the drainage/imbibition PcRI tests on two samples, showing different level of hysteresis. These plots also show how n varies with saturation on the same cycle at lower saturation levels where water resides in micropores. Thus, hysteresis in n is present even in the same cycle and it seems rock type dependent. However, the reported n values for imbibition cycle for all studied samples span in the range between 1.05 and 2.18. Note that all samples are assumed to be water-wet, because the rock samples are outcrops and mineral oil was used during the tests.

From a previous analysis of MICP pore throat size distribution, we found that most of the studied samples may possess pore size bimodality with micro-porosity; defined here as pores with less than 2 microns throat radius [23]. From the presented examples, Fig. 5 and 6, the saturation exponent values derived from drainage cycle ended by S_{wr} state is denoted by n_{dx}, drainage cycle ended by S_{wirr} state is denoted by n_d and imbibition cycle is n_{imb}. From Fig. 5, sample CO1-C shows variation in n between different saturation values on the same flooding cycle, n_{dx} and n_d. In comparison, sample IL4-B, in Fig. 6, shows relatively closer saturation index values, on the same flooding regime, at different saturation conditions. Both samples possess a range of pore sizes, however, their hysteresis response is different.

When we consider imbibition cycle, the sample which shows hysteresis with water saturation levels also shows hysteresis with flooding regime variation. For CO1-C, the saturation exponent from imbibition cycle n_{imb} is lower than from drainage, n_{dx} and n_d. This comes from the fact of having water-wet samples, that oil invades only larger pores by a piston-like displacement mechanism creating less conductive paths than imbibition where piston-like and snap-off displacements occur in large and small pores. Hence, having lower saturation exponent for imbibition is expected.

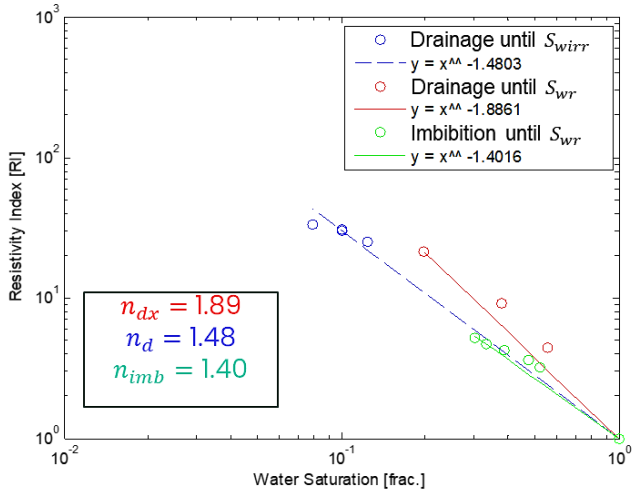

Fig. 5. Drainage and imbibition hysteresis effect on resistivity index and saturation exponent measurement for sample CO1-C.

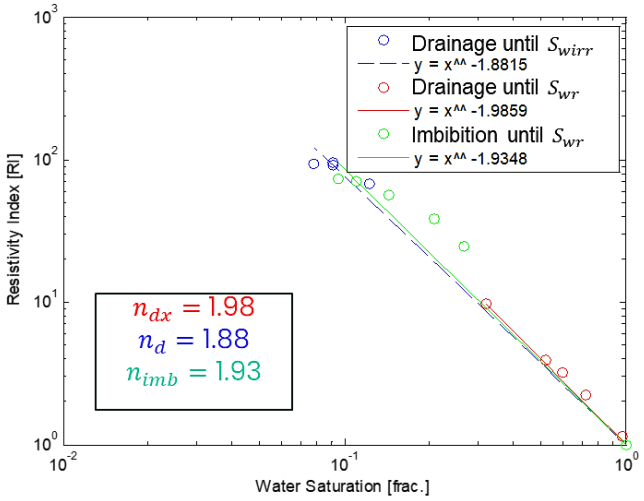

Fig. 6. Drainage and imbibition hysteresis effect on resistivity index and saturation exponent measurement for sample IL4-B.

2.2.4 Hysteresis Effect on Dielectric

As dielectric measurement is conducted outside the core flooding system and the inverted Archie exponents are independent to saturation history as in resistivity method, an instantaneous measurement after a flooding cycle is used to validate resistivity derived exponents and confirm sensitivity of dielectric measurement to flooding regimes.

Regarding the validation of Archie exponents derived from dielectric data, a prior work showed good results of $m \neq n$ dielectric Bimodal inversion to predict m and to some extent n using drainage cycle data [7]. Here in this study, we validate the Archie exponents derived from imbibition cycle dielectric data using the same core samples of the aforementioned work, and assess the effect of hysteresis on the responses of dielectric measurements.

To highlight the dielectric dispersion measurement to Archie m and n, we selected one core sample which has similar saturation level from both drainage and imbibition cycles when dielectric measurement was obtained, CO1-C, and compare the real dielectric constant dispersion with $m \neq n$ dielectric Bimodal fitting results, Fig. 7. It is observed that as the measured data set come from the same sample and saturation level, i.e. $S_w = 17\%$ and $m = 1.85$, the 1GHz dielectric response is matching between drainage and imbibition which is expected as at this frequency the dipolar polarization mechanism is dominant. Whereas there is a clear variation between drainage and imbibition data in real dielectric values at MHz range at which the interfacial polarization is dominant which is impacted by m and n. To address that the lower frequency hysteresis in dielectric response comes from different n and not from misinterpretation of m, we deliberately calculated Bimodal model with interchanged values of m and n, the resulted model response clearly doesn't fit the dielectric dispersion data and clearly the observed low frequency dielectric variation comes from hysteresis in n.

Another example illustrates the dielectric data influence to hysteresis. Here, we show the real dielectric drainage and imbibition responses on a sample which has smaller hysteresis, IL4-B, Fig. 8. The plot shows a difference in real dielectric constant curve at both low and high frequencies, but this variation resulted from having different saturation levels as implied from $m \neq n$ dielectric Bimodal fit, where dielectric data was obtained at $S_w = 10\%$ after drainage cycle and 30% after imbibition cycle. Thus, we observe from the dielectric model fit similar m and n but different S_w. Also, the plot shows the discrepancy between measured and model data when using different n from imbibition cycle.

Overall, as expected, the dielectric inverted cementation exponent matches very well, within 10% tolerance, the resistivity data obtained from fully brine saturated core analysis. Though, the drainage dielectric results show better comparison in m than imbibition dielectric data, particularly for carbonate samples which have overestimated m, Fig. 9. On the other hand, for the dielectric saturation exponent, both drainage and imbibition data show similar scattered values of n but with 10-20% tolerance, compared to resistivity PcRI method which has also some uncertainty, with no advantage to certain flooding regime, Fig. 10.

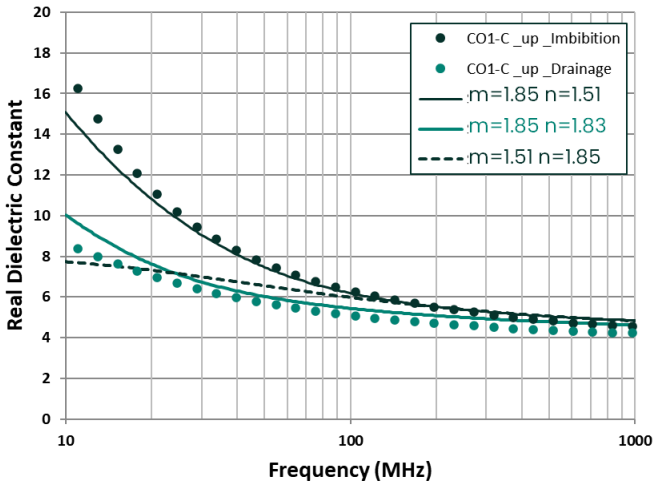

Fig. 7. Real dielectric measurement hysteresis on sample CO1-C compared with $m \neq n$ dielectric Bimodal fitting for different m and n values.

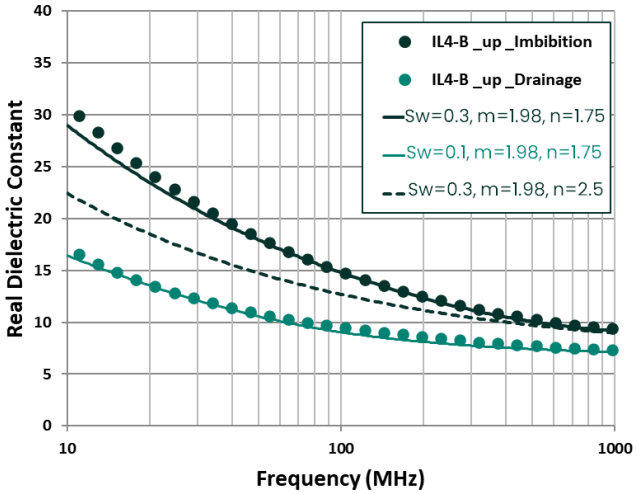

Fig. 8. Real dielectric measurement hysteresis on sample IL4-B compared with $m \neq n$ dielectric Bimodal fitting for different *Sw*, *m* and *n* values.

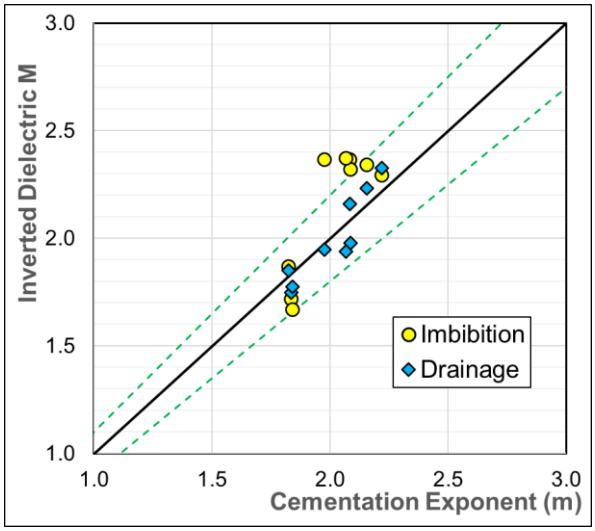

Fig. 9. Comparison between dielectric inverted cementation exponent m from both drainage and imbibition cycles, and resistivity method from fully brine saturated core samples.

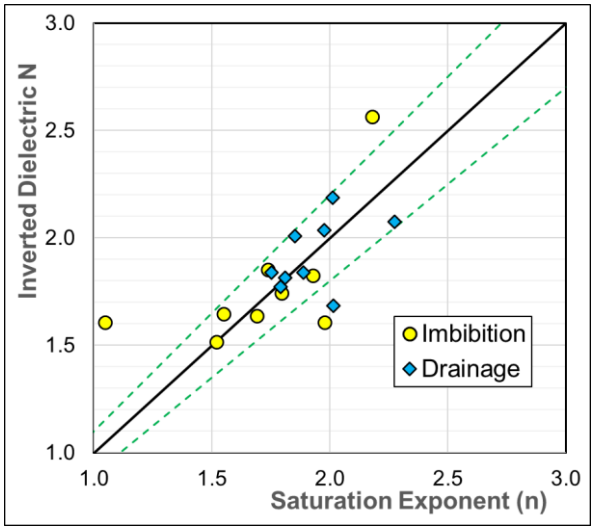

Fig. 10. Comparison between dielectric inverted saturation exponent n from both drainage and imbibition cycles, and PcRI method on the studied core samples.

3 Summary and Conclusions

In this paper, outcrop rocks and mineral oil were used to study potential impacts of the direction of fluid displacement on dielectric dispersion data by considering drainage and imbibition cycles.

An $m \neq n$ dielectric mixing model was used to invert for Archie exponents from multi-frequency dielectric data obtained from cores with drainage and imbibition displacements.

Results showed a good agreement between the derived *m* and *n* from dielectric data and the resistivity data.

As for the two-phase property *n* from the primary drainage experiment, a significant improvement is realized. The findings were consistent for different lithologies, sandstone and carbonate.

As of forced imbibition experiment, *n* exponent shows insignificant hysteresis compared to drainage results for some samples, particularly those which have no micro-porosity.

The derived *m* and *n* from imbibition dielectric experiments are comparable with that from resistivity tests, though *m* derived from dielectric data showed better results from drainage experiment compared to imbibition.

The findings of this work demonstrate the potential of using dielectric logging to derive Archie exponents in situ for enhanced formation evaluation. The application accuracy may be still subject to the degree of hysteresis between drainage and imbibition process, particularly for WBM invaded wellbore environment.

Future work is recommended to conduct both resistivity and dielectric permittivity without interrupting fluid displacement; drainage or imbibition.

The authors would like to thank Rajaa Al-Hammad of Baker Hughes for providing quality core preparation and analysis, and to Ahmed Abouzaid and Elton Frost of Baker Hughes for technical review and discussions. Stratum Reservoir Abu Dhabi laboratory is acknowledged to conduct the *PcRI* core data presented in this study.

Nomenclature

CRIM = Complex Refractive Index Model
DC = Direct Current (Zero Frequency)
MICP = Mercury Injection Capillary Pressure
NMR = Nuclear Magnetic Resonance
PcRI = Capillary Pressure Resistivity Index
RI = Resistivity Index
WBM = Water Based Mud

m = cementation exponent, unitless
n = saturation exponent, unitless
MN = dielectric inverted textural exponent when $m = n$, unitless
Rw = saturating brine resistivity, Ohm.m
Rt = formation resistivity, Ohm.m
$\emptyset$ = formation total porosity, fractions

S_w = formation water saturation, fractions
ε_{eff} = formation effective dielectric constant, Farads/m
ε_{r}' = formation real dielectric constant, unitless
ε_{r}'' = formation imaginary dielectric constant, unitless
σ = formation conductivity, S/m
ε_0 = free space dielectric constant, Farads/m
ω = angular frequency, rad/second
ε_w = water dielectric constant, unitless
ε_m = matrix dielectric constant, unitless
ε_{oil} = oil dielectric constant, unitless
$\varepsilon_{\text{fluid}}$ = fluid phase dielectric constant, unitless
ε_{dry} = dry formation dielectric constant, unitless
m^* = cementation exponent from dielectric inversion when $m \neq n$, unitless
n^* = saturation exponent from dielectric inversion when $m \neq n$, unitless

References

1. G. Archie, The Electrical Resistivity Log as an Aid in Determining Some Reservoir Characteristics. *Trans. of the AIME* **146**, 54–67 (1942)
2. A. Valori, A. Al-Ofi, W. Abdallah, M. Van Steene, C. Liu, and S. Ma, Methods and systems to determine tortuosity of rock and fluids in porous media. Patent Application US 17/429, 711 (2021)
3. J. Focke, D. Munn, Cementation exponents in Middle Eastern carbonate reservoirs. *SPE Form Eval* **2**(02), 155–167 (1987)
4. F. Kadhim, A. Samsuri, A. Kamal, A review in correlation between cementation factor and carbonate rock properties. *Life Sci J* **10**(4), 2451–2458 (2013)
5. E. Donaldson, T. Siddiqui, Relationship between the Archie saturation exponent and wettability. *SPE Form Eval* **4**(03):359–362 (1989)
6. S. Ma, A. Al-Hajari, D. Kersey, J. Funk, K. Holmes, and G. Potter, Enhanced Petrophysics: Integration of Core and Log Data for Improved Reservoir Saturation Monitoring. SPE-106350, SPE Tech Symp of Saudi Arabia Section, Dhahran, Saudi Arabia, 21-23 May (2006)
7. S. Al-Ofi, S. Ma, H. Kesserwan, G. Jin, A new approach to estimate Archie parameters m and n independently from dielectric measurements. The SPWLA 63rd annual logging symposium, Stavanger, Norway (2022)
8. A. Moss, X. Jing, J. Archer, Laboratory investigation of wettability and hysteresis effects on resistivity index and capillary pressure characteristics. *J. of Petr. Sci. and Eng.*, **24,** 2–4, (1999)
9. M. Dernaika, M. Kalam, M. Basioni, M. Svein, Hysteresis of Capillary Pressure, Resistivity Index and Relative Permeability in Different Carbonate Rock Types. *Petrophysics* **53**, 316–332, (2012)
10. S. Ma, G. Mason, & N. Morrow: "Effect of contact angle on drainage and imbibition in regular polygonal tubes," *Colloids & Surfaces, A: Physicochemical and Engineering Aspect*, **117**, pp.273 (1996)
11. N. Wardlaw, The Effects of Pore Structure on Displacement Efficiency in Reservoir Rocks and in Glass Micromodels. SPE-8843 Symposium on Enhanced Oil Recovery, Tulsa, Oklahoma, 20–23 April, (1980)
12. M. Tweheyo, Talukdar, O. Torsæter, Hysteresis Effects in Capillary Pressure, Relative Permeability and Resistivity Index of North Sea Chalk. SCA 2001-65, International Symposium of the Society of Core Analysts, Edinburgh, 17–19 September (2001)
13. P. Worthington, N. Pallatt, Effect of Variable Saturation Exponent on the Evaluation of Hydrocarbon Saturation. *SPE Form Eval* **7**, 331–336 (1992)
14. M. Hizem, H. Budan, B. Deville, O. Faivre, L. Mosse, and Simon, M., Dielectric Dispersion: A New Wireline Petrophysical Measurement. SPE-116130, the SPE Annual Technical Conference and Exhibition, Denver, Colorado, USA, 21–24 September (2008)
15. S. Forgang, A. Corley, A. Garcia, A. Hanif, F. Le, J. Jones, E. Frost Jr., S. Perry, A New Multi-Frequency Array-Dielectric Logging Service: Tool Physics, Field Testing, and Case Studies in The Permian Basin Wolfcamp Shale. SPWLA 60th Annual Logging Symp, The Woodlands, Texas, USA, 17–19 June (2019)
16. G. Jin G. Jin, S. Ma, R. Antle, & S. Al-Ofi, Reservoir characterization for isolated porosity from multi-frequency dielectric measurements. IPTC-22424, Riyadh, Saudi Arabia, 21–23 Feb (2022)
17. J.R. Birchak, C.G. Gardner, J.E. Hipp, J.M. Victor, High Dielectric Constant Microwave Probes for Sensing Soil Moisture. *Proceedings of the IEEE*, 93–98 (1974)
18. S. Al-Ofi, E. Dyshlyuk, B. Sauerer, A. Valori, F. Ali, W. Abdallah, Correlating Dielectric Dispersion Data and Wettability Index of a Carbonate Rock. SPE-192224, the SPE Kingdom of Saudi Arabia Annual Technical Symposium and Exhibition, Dammam, Saudi Arabia, 23–26 April (2018)
19. J. Baker-Jarvis, M.D Janezic, P.D. Domich, R.G. Geyer, Analysis of an Open-Ended Coaxial Probe with Lift-Off for Nondestructive Testing. *IEEE Trans. on Instr. and Meas.,* **43**(5), 711–718. (1994)
20. M. Dernaika, M.S. Efnik, M.S. Koronful, M. Al Mansoori, M.Z. Kalam, Evaluation of Water Saturation from Laboratory to Logs and the Effect of Pore Geometry on Capillarity. SPWLA-MERS-2007-F, the SPWLA Middle East Regional Symposium, Abu Dhabi, UAE, 15–19 April (2007)
21. S. Ma and M. Amabeoku, Core Analysis with Emphasis on Carbonate Rocks- Quality Assurance and Control for Accuracy and Representativeness. SEG Interpretation, February (2015)
22. E. Haslund and B. Nost, Determination of Porosity and Formation Factor of Water-Saturated Porous Specimens from Dielectric Dispersion Measurements. *Geophysics*, **63**(1), 149–153 (1998)
23. D.L. Cantrell, R.M. Hagerty, Microporosity in Arab Formation Carbonates. Saudi Arabia: *GeoArabia*, **4**(2), 129–154 (1999)